Disruption of Angiogenesis by Anthocyanin-Rich Extracts of *Hibiscus sabdariffa*

Madu Joshua[1], **Christiana Okere**[2], **O'Donnell Sylvester**[1], **Muhammad Yahaya**[1], **Omale Precious**[3], **Thagriki Dluya**[4], **Ji-Yeon Um**[5], **Musa Neksumi**[6], **Jessica Boyd**[2], **Jennifer Vincent-Tyndall**[2], **Dong-Won Choo**[7], **Diana R. Gutsaeva**[8,*], and **Wan Jin Jahng**[1,*]

[1]Petroleum Chemistry, American University of Nigeria, Yola, Nigeria

[2]Natural and Environmental Sciences, American University of Nigeria, Yola, Nigeria

[3]Industrial Chemistry, Modibbo Adama University of Technology Yola, Nigeria

[4]Biochemistry, Modibbo Adama University of Technology Yola, Nigeria

[5]Optometry, Seoul National University of Science and Technology, Seoul, Korea

[6]Chemistry, Modibbo Adama University of Technology Yola, Nigeria

[7]Bioinformatics, Korea Polytechnic Institute, Seongnam, Korea

[8]Ophtalmology, Augusta University, Augusta, GA, USA

Abstract

Abnormal vessel formations contribute to the progression of specific angiogenic diseases including age-related macular degeneration. Adequate vessel growth and maintenance represent the coordinated process of endothelial cell proliferation, matrix remodeling, and differentiation. However, the molecular mechanism of the proper balance between angiogenic activators and inhibitors remains elusive. In addition, quantitative analysis of vessel formation has been challenging due to complex angiogenic morphology. We hypothesized that conjugated double bond containing-natural products, including anthocyanin extracts from *Hibiscus sabdariffa*, may control the proper angiogenesis. The current study was designed to determine whether natural molecules from African plant library modulate angiogenesis. Further, we questioned how the proper balance of anti- or pro-angiogenic signaling can be obtained in the vascular microenvironment by treating anthocyanin or fatty acids using chick chorioallantoic membrane angiogenesis model in ovo. The angiogenic morphology was analyzed systematically by measuring twenty one angiogenic indexes using Angiogenic Analyzer software. Chick chorioallantoic model demonstrated that anthocyanin-rich extracts inhibited angiogenesis in time- and concentration-dependent manner. Molecular modeling analysis proposed that hibiscetin as a component in *Hibiscus* may bind to the active site of vascular endothelial growth factor receptor 2 (VEGFR2) with G= −8.42 kcal/mol of binding energy. Our results provided the evidence that

*Address correspondence to: Wan Jin Jahng, Ph.D. Retina Proteomics Laboratory, Department of Petroleum Chemistry, American University of Nigeria, Yola, Nigeria, Tel: +234-805-550-1032; wan.jahng@aun.edu.ng; Diana R. Gutsaeva, Ph.D. Ophtalmology, Augusta University, Augusta, GA, USA, Tel: +1 706 721 7910, dgutsaeva@augusta.edu.

anthocyanin is an angiogenic modulator that can be used to treat uncontrolled neovascular-related diseases, including age-related macular degeneration.

Keywords

age-related macular degeneration; angiogenesis; anthocyanin; chick embryo; chorioalantoic membrane; fatty acid; *Hibiscus sabdariffa*; molecular modeling; VEGFR; vessel formation

Introduction

Balanced blood vessel formation corresponds to the assembly of angioblasts, vessel sprouting, recruiting pericytes and endothelial smooth muscle cells to form tubes, branches, and capillary blood vessels from the existing vascular network [1–4]. Uncontrolled angiogenic reactions are the major pathological components of the late stage of wet age-related macular degeneration (AMD) when abnormal blood vessels develop toward into the macular. Pathological angiogenesis is also seen in other inflammatory diseases, ischemic conditions, diabetic neuropathy, and cancer, thus disruption of angiogenesis has become a promising target for therapies to stop diseases that thrive on angiogenesis. However, the molecular mechanism of the proper balance between angiogenic activators and inhibitors remains unknown. In addition, systematic analysis of angiogenesis has been challenging due to complex vessel morphology that includes vessel length, branches, nodes, and segments.

Here, we propose that natural compounds containing aromatic rings with a carbohydrate moiety in plant library, may regulate blood vessel formation through the inhibition of angiogenesis. The current study was designed to determine the time and dose-dependent modulation of angiogenesis by anthocyanin and how the proper analysis could be performed using systematic calculations.

Previously, our proteomic data demonstrated that early signaling molecules, including erythropoietin, prohibitin, PP2A, vimentin, HIF1, JAK2, and nitric oxide, are involved in apoptosis and angiogenesis in the retina and the RPE, and imbalance of oxidative environment may lead to the initiation of AMD [5–11]. Here, we aimed to use specific natural compound library to regulate the early signaling targets to modulate blood vessel formation processes. The therapeutic role of *Hibiscus sabdariffa* calyx was examined and its extracts linked to its phytochemical constituents including anthocyanin (>100 mg cyanidine rutinoside/100 g plants) were determined [12,13]. We established 21 angiogenic index, including vessel length, branches, nodes and segments, using Angiogenesis Analyzer software. Quantitative analysis showed that anthocyanin inhibited 50–80 % of blood vessels formation. As angiogenic activators, selected fatty acid mixtures that include oleic (18:1), linoleic (18:2, w6), linolenic (18:3, w3), palmitic (16:0), and palmitoleic (16:1) acid, significantly stimulated angiogenesis by 20–50 %. Our data suggest that natural chromophore from edible plants library may regulate the vessel formation in time- and dose-dependent manner. Protein-ligand docking analysis using SwissDock software proposed that hibiscetin from Hibiscus may bind to the active site of Vascular endothelial growth factor receptor 2 (VEGFR2) with the Asp1046, Cys1045, Cys919, and Glu917 showing ΔG= −8.62 kcal/mol of binding energy. The current study implies that anthocyanin rich extract of

H. sabdariffa has an anti-angiogenic effect in ovo and may be a potential candidate for the treatment of angiogenic diseases.

MATERIALS AND METHODS

Methods

We followed the NIH Guide and the Association for Research in Vision and Ophthalmology (ARVO) statement for in vivo experiments. Avian embryos are not considered live animals under PHS policy. The use of chicken embryos at gestation day 12 and younger does not require an ACUC Animal Use Protocol Application. Chick embryos younger than embryonic day 13 (E13) are assumed unable to experience pain. Therefore, E13 and younger embryos were euthanized by hypothermia, typically conducted by placing the eggs in a −20°C freezer or < 4°C for 4 hours. Embryonic death was confirmed by decapitation, membrane disruption, or maceration. Chick embryos between E13 – E17 can experience pain and were euthanized by cervical dislocation.

All experiments were repeated with many biological samples (n >3) with technical triplicate (n > 9). Stat View software was used for statistical analysis. Statistical significance was analyzed using unpaired Students' test or variance (ANOVA) when appropriate. The significance level $P < 0.05$ is considered as statistically significant.

Collection of Plant Materials

Air dried anthocyanin-containing plants library, including Hibiscus sabdariffa calyx, Moringa oleifera, Habiscus asper, Vernonia amygdalina, Elaeis guineensis, Manihot esculenta, Chrysanthemum moriflium, Sesamum radiatum, Balanite aegyptica, Talinum triangulare and Telfairia occidentalis was obtained locally from Yola, Nigeria. It was taxonomically identified and authenticated using three different African plant databases (http://www.gbif.org/resource/81181; http://posa.sanbi.org/intro_precis.php; http://www.africanplants.senckenberg.de/root/index.php).

Extraction of Anthocyanin

H. sabdariffa calyx extracts were obtained by soaking 100 g of the powder in 1.8 L of distilled water for 12 hours, followed by filtering the mixture using filter paper (pore size 11 μm). The filtrate was collected and the residue rinsed with 200 mL of distilled water. The filtrate was lyophilized and used for the current study. Anthocyanin concentrations, both total and monomeric, were determined quantitatively by pH differential method. Anthocyanin content was calculated as mg cyanidin-glucoside equivalent/100 g of solid sample ($ε = 28840$ $M^{-1}cm^{-1}$) [12,13]. Fatty acids (unsaturated fatty acid: saturated fatty acids = 85:15, oleic/linoleic-linolenic/palmitolic/palmitic/stearic acid) were tested as pro-angiogencic molecules [14,15].

Inoculation of Chick Embryo with Anthocyanin

Freshly prepared H. sabdariffa calyx extracts (dissolved in Ringer's solution or PBS or ddH$_2$O) 14 μg or 58 μg concentrations were injected in fertilized eggs (average 38 g, chick embryo, Gallus domesticus) at 0, 2, 4, 7, and 9 days (pre-incubation) and were incubated at

37.5 °C for additional 4, 5, 7, 15 days (post-incubation) in humidified incubator. Angiogenic indexes such as vessel length, branches, nodes and segments were determined upon treatment with anthocyanin. The experiments were repeated 20 times to determine time and dose - dependent vessel formation on anthocyanin treatment. Each experiment includes 7 - 30 chick embryos/set/week and a total of 212 chick embryos were used and 345 vessel images were obtained. Pre-incubation day ED = 0–4 days and Post-incubation day ED = 4–10 days were mainly tested against control sample that contains the same amount of Ringer solution.

Angiogenic Analysis of Chick Embryo Chorioalatoic Membrane

Twenty one angiogenic parameters were tested using Angiogenesis Analyzer macro connected Image J software (Gilles Carpentier, http://image.bio.methods.free.fr/ImageJ/?Angiogenesis-Analyzer-for-ImageJ). Vessel formation of anthocyanin-treated chick embryo with pre-incubation (0–2 days) and post-incubation (4–7 days, anthocyanin + = 14 μg, and anthocyanin ++ = 58 μg/chick embryo) was analyzed. Angiogenic Analysis showing extremities (A1-B1); nodes identified as 3 neighbor (A2-B2); twig (C1, D1), segment (C2, D2) delimited by two junctions (C3, D3) and branch (C4, D4). E shows a junction implicated only in branch (E1) and master junctions like E2 delimiting master segments (E3). F represents the master tree composed from master segments associated by master junctions delimiting the meshes (F1). Two close master junctions can be fused into a unique master junction (F2) and the underlying segment (F3).

Molecular Modeling

A 3D model of the protein was built using the 3D structure VEGFR2 as a template and selected ligands, including malvidin 3-galatoside, cyanidin, cyaniding 6-glucoside, and hibiscetin [16–18]. A random selected non-VEGFR2 binding molecules, including alanine, D-glucose, and oxalic acid were used as negative controls (data not shown).

Vascular endothelial growth factor receptor 2 (VEGFR2) was obtained from the Protein Data Bank. Protein-ligand docking server, including SwissDock and GOLD (version 5.0), was used for ligand-protein interaction studies (http://www.swissdock.ch/docking#). The active site of VEGFR2 and protein structure were examined among seven X-ray diffraction crystal structures (PDB ID = 1Y6A, 1Y6B, 1YWN, 2OH4, 2P2H, 2P21, 2QU5). The conserved amino acid residues presenting the VEGFR2 active site were L840, V848, C866, K868, E885, V899, V916, E917, F918, C919, K920, G922, L1035, C1045, D1046 and F1047.

SwissDock predicted the molecular interaction between VEGFR2 and selected anthocyanin molecules, including hibiscetin. SwissDock contains a database of proteins and ligand structures. SwissDock generated many binding modes using EADock software as local docking in the box as well as blind docking in the vicinity of all VEGFR2 cavities. At the same time, binding energies were calculated and the most favorable energies were evaluated to show the most favorable clusters. 257 bindings were calculated with clusters (0–37), elements (0–15), FullFitness (−1588.73 to −1567.50 kcal/mol), binding energy ΔG (−8.42 to −6.20 kcal/mol). SwissDock used a hybrid evolutionary algorithm with two fitness functions, with the CHARMM package for energy calculations.

RESULTS

Anti-angiogenic effect of anthocyanin rich extract of *Hibiscus sabdariffa*

First, we tested the following air dried anthocyanin-containing plants as an initial library, including *Hibiscus sabdariffa calyx, Moringa oleifera, Habiscus asper, Vernonia amygdalina, Elaeis guineensis, Manihot esculenta, Chrysanthemum moriflium, Sesamum radiatum, Balanite aegyptica, Talinum triangulare* and *Telfairia occidentalis*, obtained locally in Yola, Nigeria (Figure 1). Freshly prepared Hibiscus extracts (dissolved in Ringer's solution or ddH$_2$O) were injected in fertilized eggs (*Gallus domesticus*) at 0, 2, 4, 7, and 9 days and were incubated at 37.5 °C for additional 4, 5, 7, 15 days [19]. The altered angiogenesis upon anthocyanin treatment was analyzed by angiogenic indexes. Pre-incubation embryonic day (ED) = 0, 2, 4, 9 days and post-incubation embryonic day ED = 4, 7, 9, 10, 17, 19 days were examined to determine the time-dependent inhibition.

The inhibitory effect of anthocyanin (>100 mg cyanidin glucoside/100 g plant) was determined using 14 μg and 58 μg extract/38 g chick embryo (Figure 2A). Anthocyanin-treated chick embryo group I (14 μg anthocyanin/chick embryo) showed decreased vessel formation compared to the vehicle-only control when it was administered at pre-incubation embryonic day (ED) = 2 and analyzed at post-injection embryonic day 8 (ED = 10). Higher concentration of anthocyanin-treated group II (58 μg anthocyanin /38 g chick embryo) significantly inhibited blood vessel formation compared to vehicle-only control or lower concentration of anthocyanin group I. Other kinetic time point, including pre-incubation ED = 4 and post-injection ED = 6, was examined (Figure 2B). At ED = 10 chick embryo was harvested and vessel formation was analyzed. Our results demonstrated that increased concentration of anthocyanin rich extract led to significant decrease in the angiogenic index determined through counting the number of blood vessel branch points. We observed maximum inhibition of blood vessels formation at embryonic day ED = 2 compared to treatment at later stage (pre-incubation ED> 10 days). When anthocyanin was administered at later stage with pre-incubation ED = 9 and post-injection ED = 8, no phenotypical differences were observed (Figure 2C). To determine early time-dependent anti-angiogenic index by anthocyanin extract, we injected anthocyanin at pre-incubation day ED = 0 and post-incubation day ED = 4. Angiogenic index showed 60 % inhibition of vessel length growth compared to control (Figure 3) supporting the hypothesis that early treatment (ED = 0) of anthocyanin on the embryo significantly (p< 0.05) inhibited blood vessel length growth compared to the control.

Angiogenic Index Analysis

Next, to determine the angiogenic morphology systematically, we measured twenty one angiogenic index using Angiogenic Analyzer macro (Gilles Carpentier, http://image.bio.methods.free.fr/ImageJ/?Angiogenesis-Analyzer-for-ImageJ) on anthocyanin-treated verses control chick embryo (chorioallantoic membrane) (Figure 4A). The Angiogenic Analyzer detects vessel networks and analyzes the vascular organization of endothelial cells. To evaluate the anti-angiogenic effects of selected molecules, the Analyzer obtains a quantitative evaluation of the vessel network by extracting characteristic information of the angiogenic images. Parameters analyzed were inhibited by anthocyanin

treated chick embryo (anthocyanin + = 14 μg anthocyanin and anthocyanin ++ = 58 μg anthocyanin/38 g chick embryo), compared to the control (Figure 4B). We determined the angiogenic parameters, including extremities, nodes, junctions, master junction, master segments, master segments length, meshes, total meshes area, number of segments, isolated elements and branches, number of segments, branches, number of isolated elements, total length, total branching length, total segments length, total branches length, total isolated branches length, branching interval, total segments length /branches, mesh index, master segments length /master segments and mean mesh size. Next, we examined Angiogenesis Analyzer to obtain angiogenic index quantitatively (Figure 5). Systematic analysis showed extremities (A1-B1), nodes identified as 3 neighbor (A2-B2), twig (C1, D1), segment (C2, D2) delimited by two junctions (C3, D3), and branch (C4, D4). E shows a junction implicated only in branch (E1) and master junctions like E2 delimiting master segments (E3). F represents the master tree composed from master segments associated by master junctions delimiting the meshes (F1). Two close master junctions can be fused into a unique master junction (F2) and the underlying segment (F3).

Fatty Acids as an Angiogenic Stimulators

Fatty acids that include eicosanoid may serve as effective pro-angiogenic factors, considering that fatty acids regulate vascular endothelial cell proliferation, migration and capillary formation [14]. Anti-angiogenic anthocyanin was compared to selected fatty acids mixtures as angiogenic stimulator (Figure 6). Fatty acids, including oleic (18:1), linoleic (18:2, w6), linolenic (18:3, w3), palmitic (16:0), palmitoleic (16:1), up-regulated vessel length and branches 20–50%, compared to control. Ten major angiogenic indexes, that includes extremities, nodes, junctions, master junction, number of master segments, meshes, total meshes area, number of segments, branches and number of isolated segments, was measured to show the pro-angiogenic effects of fatty acids (Figure 7A). Total isolated branch length increased 70% when fatty acids mixtures were injected to chick embryo (Pre-incubation ED = 2, post-injection ED = 8, total ED = 10 days), whereas branching interval was not changed (Figure 7B). Mean mesh size, total master segments length, total length, total branching length, total segments length, and total branches length were up-regulated (Figure 7C).

Molecular Modeling

A 3D model of the protein-ligand interaction was built using the 3D structure of VEGFR2 as a template and selected anthocyanin as a ligand. VEGFR2 was obtained from the Protein Data Bank [20,21]. Six molecules, including cyaniding-3-glucoside and hibiscetin from *Hibiscus* were selected for protein-ligand modeling analysis (Figure 8a) [22–24].

The conserved residues presenting VEGFR2 active sites were A866, L840, K920, F918, G922, C919, E917, V848, C1045, F1047, L1035, G922, K920, D1046, V916, V899, K868, and E885. The modeling was performed using SwissDock. SwissDock generated many binding modes using EADock software as local docking in the box as well as blind docking in the vicinity of all VEGFR2 cavities. At the same time, binding energies (G) were calculated and the most favorable energies were evaluated to show the most favorable

clusters. Total 257 binding were calculated with clusters (0–37), elements (0–15), FullFitness (−1588.73 to −1567.50 kcal/mol), binding G (−8.42 to −6.20 kcal/mol).

The 10 conserved hydrophobic amino acids in receptor tyrosin kinases including A866, L840, F918, G922, V848, F1047, L1035, G922, V916, and V899 in the active site of VEGFR2, were proposed to interact with three aromatic rings of hibiscetin by forming hydrophobic interaction and π–π interaction (Figure 8b). Other conserved amino acids seem to contribute to forming hydrogen bonding between K920, C919, E917, C1045, K920, D1046, K868, and E885 and 7 hydroxyl groups of hibiscetin. Trihydroxylphenyl ring of hibiscetin interacts with C1045 and D1046 through hydrogen bonding whereas the other two aromatic ring fitted in the hydrophobic pocket of the active site. Hibiscetin contains seven hydrogen bond donor sites and nine hydrogen bond acceptor atoms. Trihydroxyphenyl group is perpendicular to the chromenone structure, thus all three aromatic rings fit into the hydrophobic pocket of VEGFR2.

The molecular mechanism of the proper balance between angiogenic activation and inhibition remains elusive. The current study was designed to investigate whether natural antiangiogenic molecules modulate angiogenesis and how the proper balance of pro- and anti-angiogenic signaling can be analyzed using a chick embryo model [19,25]. Our data demonstrated that systematic administration of anthocyanin-rich extracts of Hibiscus plant blocked collagenolytic activity *in ovo*, leading to a significant reduction of vessel formation of chick embryo. Systematic analysis of angiogenic index demonstrated that the hierachical branching pattern of vessel formation exists in the chorioallantoic membrane (CAM) and both global as well as local organization of the vascular network characterizes angiogenesis. Further, the current study introduced the systematic analysis of angiogenic index using the Angiogenesis Analyzer that detects vessel networks and analyzes the vascular organization of endothelial cells. To evaluate the angiogenic effects of anthocyanin and fatty acids, the Angiogenesis Analyzer obtains a quantitative evaluation of the vessel network by extracting characteristic information of the angiogenic images [26].

Previously, our proteomic studies under stress conditions identified the following molecular changes in apoptotic and angiogenic reactions in the retina and RPE that include (1) mitochondrial dysfunction in the peripheral RPE in AMD, (2) oxidative stress by intense (> 7,000 lux) and constant light(> 1 week), (3) cytoskeletal remodeling by actin, vimentin, and tubulin under stress, (4) high concentration of nitric oxide, (5) hypoxia, (6) disrupted circadian clock, (7) erythropoietin changes via pJAK2, pSTAT3, Bclxl, HIF1, VEGFR (8) altered lipid concentrations, (9) altered retinoid metabolism (RPE65,CRALBP), (10) altered energy metabolism by S/T/Y kinases, creatine kinase, pyruvate kinase (11) altered expressions of heat shock proteins, crystallins [6,8,9,27]. Based on our proteomic data, we tested the following molecules as anti-apoptotic and anti-angiogenic molecules: (1) prohibitin as an anti-apoptotic mitochondrial-nuclear shuttle), (2) erythropoietin as an anti-apoptotic protein via JAK2/STAT3 pathway, (3) melatonin as an anti-apoptotic, anti-angiogenic molecule,and a circadian determinant protecting cytoskeletal reorganization through PP2A/vimentin pathway, (4) okadaic acid, arginine, and SNAP (nitric oxide generator) to regulate nitric oxide concentration, (5) changes in certain lipids, including

cardiolipin and cholesterol as specific biomarkers of apoptotic retina and RPE under stress conditions [10].

The chorioallantoic membrane in a chick embryo model offers a number of unique advantages to study the complex, multistep process of angiogenesis [19]. The chorioallantoic membrane provides a supportive environment for a source of angiogenic blood vessels. The chorioallantoic membrane comprises the fully developed ectoderm capillary plexus which is a network of tiny capillaries connecting the arterial and venous blood vessel networks. Late injection (t = 10–15 days of pre-incubation) of anthocyanin has less influence than early injection (t = 0 to 4 days pre-incubation). Fatty acids up-regulated vessel length (20–30%) and isolated branches (50%), respectively.

At the later stage, CAM assay represents the certain disadvantage because it may contain a pre-developed vascular network and the vasodilation that invariably follows its manipulation may be hard to distinguish from the effects of the test substance.

Hibiscus sabdariffa is identified as an annual red Sorrel dicotyledonous plant. It is an herbaceous tropical plant containing anthocyanin, flavonoids and polyphenol acids which includes cyanidin-3-sambubioside, delphinidin-3-O-glucoside and delphinidin-3-O-sambubioside. Historically *sabdariffa* extract has been used for treating liver disorders, hypertension, pyrexia, diuretic, emollient and purgative. The calyx mixtures decrease intestinal transit, and exert anti-inflammatory and anti-mutagenic effects. Its beneficial effects are linked to the presence of phytochemical constituents including anthocyanin which is the most abundant (>100 mg cyanidine rutinoside/100 g plants).

Anthocyanin is a mixture of glycosylated polyhydroxy and polymethoxy flavonoids. Anthocyanin has characteristic carbon structures containing three aromatic rings with one glucoside. Bright red-orange color produced under acidic condition is due to the positive charge on heterocyclic oxygen of conjugated chromophore. Naturally occurring anthocyanin includes cyanidin, delphinidin, malvidin, pelargonidin, peonidin, petunidin, and hibiscetin. Dietary anthocyanins possess strong antioxidant activity to scavenge reactive oxygen species (ROS) such as superoxide, singlet oxygen, peroxide, hydrogen peroxide and hydroxyl radical.

A 3D model of the protein-ligand interaction was built using the 3D structure of VEGFR2 as a template and selected anthocyanin as a ligand. VEGFR2 was obtained from the Protein Data Bank [20,21]. Six molecules, including cyaniding-3-glucoside and hibiscetin from *Hibiscus* were selected for protein-ligand modeling analysis (Figure 8a) [22–24]. The conserved residues presenting VEGFR2 active sites were A866, L840, K920, F918, G922, C919, E917, V848, C1045, F1047, L1035, G922, K920, D1046, V916, V899, K868, and E885. The modeling was performed using Swissdock. SwissDock generated many binding modes using EADock software as local docking in the box as well as blind docking in the vicinity of all VEGFR2 cavities. At the same time, binding energies were calculated and the most favorable energies were evaluated to show the most favorable clusters. Total 257 binding were calculated with clusters (0–37), elements (0–15), FullFitness (−1588.73 to −1567.50 kcal/mol), binding energy G (−8.42 to −6.20 kcal/mol).

The 10 conserved hydrophobic amino acids, including A866, L840, F918, G922, V848, F1047, L1035, G922, V916, and V899 in the active site of VEGFR2, were proposed to interact with three aromatic rings of hibiscetin by forming hydrophobic interaction and π–π interaction (Figure 8b). Other conserved amino acids seem to contribute to forming hydrogen bonding with K920, C919, E917, C1045, K920, D1046, K868, and E885 and hydroxyl group of hibiscetin. Trihydroxyphenyl ring of hibiscetin interacts with C1045 and D1046 through hydrogen bonding whereas the other two aromatic ring fitted in the hydrophobic pocket of the active site. Hibiscetin contains seven hydrogen bond donor sites and nine hydrogen bond acceptor atoms.

The current study determined 21 angiogenic indexes, including vessel length, branches, nodes and segments, using angiogenesis analyzer to show 50–60 % inhibition of blood vessels formation by anthocyanin rich extract of *H. sabdariffa*. Our results also revealed that selected fatty acid mixtures that include oleic (18:1), linoleic (18:2, w6), linolenic (18:3, w3), palmitic (16:0), and palmitoleic (16:1) acid, significantly stimulated angiogenesis by 20–50 %. Our data suggest that conjugated double bond-containing natural products from sub-Saharan African plants library may regulate the vessel formation in time- and dose-dependent manner. Our studies imply that potential molecular determinants including anthocyanin may inhibit angiogenesis and the proper balance of pro- and anti-angiogenic signaling may control the vascular microenvironment. The current study demonstrated that anthocyanin rich extract of *H. sabdariffa* has anti-angiogenic effect *in vivo* and may be a potential candidate for the treatment of angiogenic diseases, including wet AMD.

Conclusion

The current study examined the anthocyanin-rich Hibiscus extracts to determine their time- and dose-dependent anti-angiogenic properties using chick chorioallantoic membrane model in ovo. Using this well-characterized model we showed that anthocyanin-rich extracts inhibited angiogenesis in time and concentration-dependent manner showing maximum inhibition of vessel formation in early treatment on 0–2 pre-incubation days. Quantitative determination of angiogenesis using 21 angiogenic indexes provided the evidence that *Hibiscus sabdariffa* inhibits angiogenesis and therefore can be used for treating uncontrolled angiogenesis-related diseases, including wet AMD. Imbalance between angiogenic stimulators and inhibitors may lead to incomplete vessel maturation. Our data suggest that angiogenic determinants that include fatty acids and anthocyanin as well as their concentration, pre-incubation timing and injection timing may exist in neovasculogenesis and angiogenesis.

Acknowledgments

References

1. Folkman J. Anti-angiogenesis: new concept for therapy of solid tumors. Ann Surg. 1972; 175:409–416. DOI: 10.1097/00000658-197203000-00014 [PubMed: 5077799]
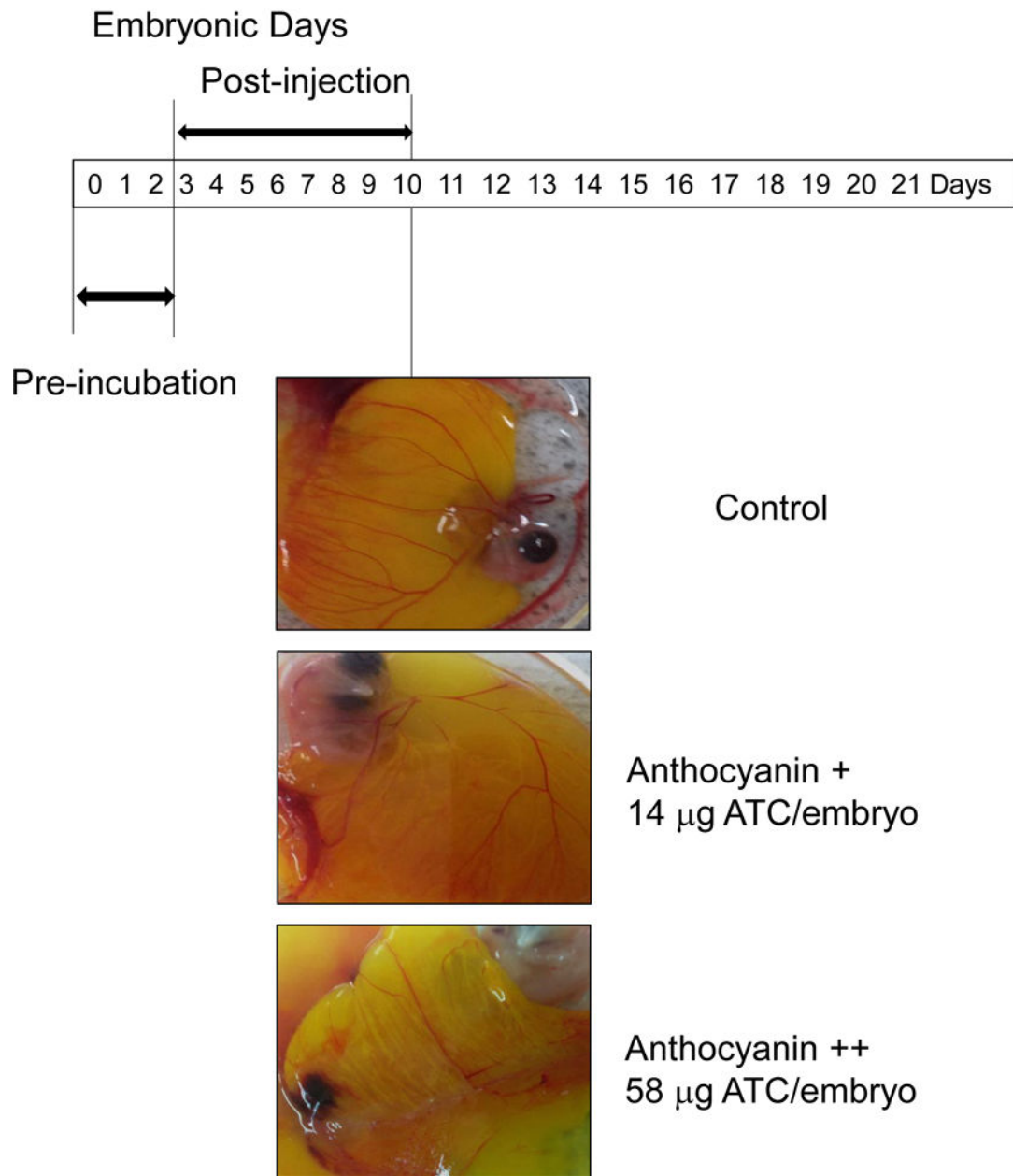
2. Shweiki D, Itin a, Neufeld G, Gitay-Goren H, Keshet E. Patterns of expression of vascular endothelial growth factor (VEGF) and VEGF receptors in mice suggest a role in hormonally regulated angiogenesis. J Clin Invest. 1993; 91:2235–2243. DOI: 10.1172/JCI116450 [PubMed: 7683699]

3. Zuluaga MF, Mailhos C, Robinson G, Shima DT, Gurny R, Lange N. Synergies of VEGF inhibition and photodynamic therapy in the treatment of age-related macular degeneration. Invest Ophthalmol Vis Sci. 2007; 48:1767–1772. DOI: 10.1167/iovs.06-1224 [PubMed: 17389510]

4. Markovets AM, Fursova AZ, Kolosova NG. Therapeutic action of the mitochondria-targeted antioxidant SkQ1 on retinopathy in OXYS rats linked with improvement of VEGF and PEDF gene expression. PLoS One. 2011; 6:1–8. DOI: 10.1371/journal.pone.0021682

5. Sripathi SR, He W, Atkinson CL, Smith JJ, Liu Z, Elledge BM, Jahng WJ. Mitochondrial-nuclear communication by prohibitin shuttling under oxidative stress. Biochemistry. 2011; 50:8342–51. DOI: 10.1021/bi2008933 [PubMed: 21879722]

6. Sripathi SR, Sylvester O, He W, Moser T, Um JY, Lamoke F, Ramakrishna W, Bernstein PS, Bartoli M, Jahng WJ. Prohibitin as the Molecular Binding Switch in the Retinal Pigment Epithelium. Protein J. 2015; doi: 10.1007/s10930-015-9641-y

7. Lee H, Arnouk H, Sripathi S, Chen P, Zhang R, Bartoli M, Hunt RC, Hrushesky WJM, Chung H, Lee SH, Jahng WJ. Prohibitin as an oxidative stress biomarker in the eye. Int J Biol Macromol. 2010; 47:685–90. DOI: 10.1016/j.ijbiomac.2010.08.018 [PubMed: 20832420]

8. Arnouk H, Lee H, Zhang R, Chung H, Hunt RC, Jahng WJ. Early biosignature of oxidative stress in the retinal pigment epithelium. J Proteomics. 2011; 74:254–61. DOI: 10.1016/j.jprot.2010.11.004 [PubMed: 21074641]

9. Chung H, Lee H, Lamoke F, Hrushesky WJM, Wood Pa, Jahng WJ. Neuroprotective role of erythropoietin by antiapoptosis in the retina. J Neurosci Res. 2009; 87:2365–74. DOI: 10.1002/jnr.22046 [PubMed: 19301424]

10. Zhang R, Hrushesky WJM, Wood Pa, Lee SH, Hunt RC, Jahng WJ. Melatonin reprogrammes proteomic profile in light-exposed retina in vivo. Int J Biol Macromol. 2010; 47:255–60. DOI: 10.1016/j.ijbiomac.2010.04.013 [PubMed: 20434483]

11. Sripathi SR, He W, Um J, Moser T, Dehnbostel S, Kindt K, Goldman J, Frost MC, Jahng WJ. Nitric oxide leads to cytoskeletal reorganization in the retinal pigment epithelium under oxidative stress, 2012. 2012:1167–1178.

12. Obouayeba AP, Djyh NB, Diabate S, Djaman AJ, N'Guessan JD, Kone M, Kouakou TH. Phytochemical and antioxidant activity of roselle (Hibiscus Sabdariffa L.) petal extracts. Res J Pharm Biol Chem Sci. 2014; 5:1453–1465.

13. Lee CH, Kuo CY, Wang CJ, Wang CP, Lee YR, Hung CN, Lee HJ. A polyphenol extract of Hibiscus sabdariffa L. ameliorates acetaminophen-induced hepatic steatosis by attenuating the mitochondrial dysfunction in vivo and in vitro. Biosci Biotechnol Biochem. 2012; 76:646–51. DOI: 10.1271/bbb.110579 [PubMed: 22484925]

14. Basak S, Das MK, Duttaroy AK. Fatty acid-induced angiogenesis in first trimester placental trophoblast cells: Possible roles of cellular fatty acid-binding proteins. Life Sci. 2013; 93:755–762. DOI: 10.1016/j.lfs.2013.09.024 [PubMed: 24095946]

15. Park JM, Kwon SH, Han YM, Hahm KB, Kim EH. Omega-3 polyunsaturated Fatty acids as potential chemopreventive agent for gastrointestinal cancer. J Cancer Prev. 2013; 18:201–8. DOI: 10.15430/jcp.2013.18.3.201 [PubMed: 25337547]

16. McTigue MA, Wickersham JA, Pinko C, Showalter RE, Parast V C, Tempczyk-Russell A, Gehring MR, Mroczkowski B, Chen-Chen K, Villafranca JE, Appelt K. Crystal structure of the kinase domain of human vascular endothelial growth factor receptor 2: A key enzyme in angiogenesis. Structure. 1999; 7:319–330. DOI: 10.1016/S0969-2126(99)80042-2 [PubMed: 10368301]

17. McTigue M, Murray BW, Chen JH, Deng YL, Solowiej J, Kania RS. Molecular conformations, interactions, and properties associated with drug efficiency and clinical performance among VEGFR TK inhibitors. Proc Natl Acad Sci U S A. 2012; 109:18281–18289. DOI: 10.1073/pnas.1207759109 [PubMed: 22988103]

18. Xia Y, Song X, Li D, Ye T, Xu Y, Lin H, Meng N, Li G, Deng S, Zhang S, Liu L, Zhu Y, Zeng J, Lei Q, Pan Y, Wei Y, Zhao Y, Yu L. YLT192, a Novel, Orally Active Bioavailable Inhibitor of

VEGFR2 Signaling with Potent Antiangiogenic Activity and Antitumor Efficacy in Preclinical Models. Sci Rep. 2014; 4:6031.doi: 10.1038/srep06031 [PubMed: 25112436]

19. Brooks PC, Silletti S, Schalscha TL von, Friedlander M, Cheresh Da. Disruption of Angiogenesis by PEX, a Noncatalytic Metalloproteinase Fragment with Integrin Binding Activity. Cell. 1998; 92:391–400. DOI: 10.1016/S0092-8674(00)80931-9 [PubMed: 9476898]

20. De Maria F, Pedersen JZ, Caccuri AM, Antonini G, Turella P, Stella L, Lo Bello M, Federici G, Ricci G. The specific interaction of dinitrosyl-diglutathionyl-iron complex, a natural NO carrier, with the glutathione transferase superfamily: suggestion for an evolutionary pressure in the direction of the storage of nitric oxide. J Biol Chem. 2003; 278:42283–93. DOI: 10.1074/jbc.M305568200 [PubMed: 12871945]

21. Hagström L, Agbulut O, El-Hasnaoui-Saadani R, Marchant D, Favret F, Richalet J-P, Beaudry M, Launay T. Epo is relevant neither for microvascular formation nor for the new formation and maintenance of mice skeletal muscle fibres in both normoxia and hypoxia. J Biomed Biotechnol. 2010; 2010:137817.doi: 10.1155/2010/137817 [PubMed: 20414335]

22. Lee CH, Kuo CY, Wang CJ, Wang CP, Lee YR, Hung CN, Lee HJ. A Polyphenol Extract of Hibiscus sabdariffa L. Ameliorates Acetaminophen-Induced Hepatic Steatosis by Attenuating the Mitochondrial Dysfunction in Vivo and in Vitro. Biosci Biotechnol Biochem. 2012; 76:646–651. DOI: 10.1271/bbb.110579 [PubMed: 22484925]

23. Da-Costa-Rocha I, Bonnlaender B, Sievers H, Pischel I, Heinrich M. Hibiscus sabdariffa L. - A phytochemical and pharmacological review. Food Chem. 2014; 165:424–443. DOI: 10.1016/j.foodchem.2014.05.002 [PubMed: 25038696]

24. Mahadevan N, Kamboj S, Kamboj P. Hibiscus sabdariffa Linn. – An overview. Nat Prod Radiance. 2009; 8:77–83.

25. Lokman, Na, Elder, ASF., Ricciardelli, C., Oehler, MK. Chick Chorioallantoic Membrane (CAM) Assay as an In Vivo Model to Study the Effect of Newly Identified Molecules on Ovarian Cancer Invasion and Metastasis. Int J Mol Sci. 2012; 13:9959–70. DOI: 10.3390/ijms13089959 [PubMed: 22949841]

26. Jain RK. Molecular regulation of vessel maturation. Nat Med. 2003; 9:685–693. DOI: 10.1038/nm0603-685 [PubMed: 12778167]

27. Lee H, Chung H, Lee SH, Jahng WJ. Light-induced phosphorylation of crystallins in the retinal pigment epithelium. Int J Biol Macromol. 2011; 48:194–201. DOI: 10.1016/j.ijbiomac.2010.11.006 [PubMed: 21094180]

Figure 1.
Sub-Saharan African plants library. Thirteen edible medicinal plants containing anthocyanin were collected locally in Yola, Nigeria. *Hibiscus sabdariffa calyx, Moringa oleifera, Habiscus asper, Vernonia amygdalina, Elaeis guineensis, Manihot esculenta, Chrysanthemum moriflium, Sesamum radiatum, Balanite aegyptica, Talinum triangulare and Telfairia occidentalis* were identified taxonomically and authenticated using African Plants Databases. Preliminary plants screening showed that *Hibiscus sabdariffa* has an inhibitory effect on angiogenesis.

A.

Embryonic Days

Post-injection

| 0 1 2 | 3 4 5 6 7 8 9 10 | 11 12 13 14 15 16 17 18 19 20 21 Days |

Pre-incubation

Control

Anthocyanin +
14 μg ATC/embryo

Anthocyanin ++
58 μg ATC/embryo

B.

Post-injection
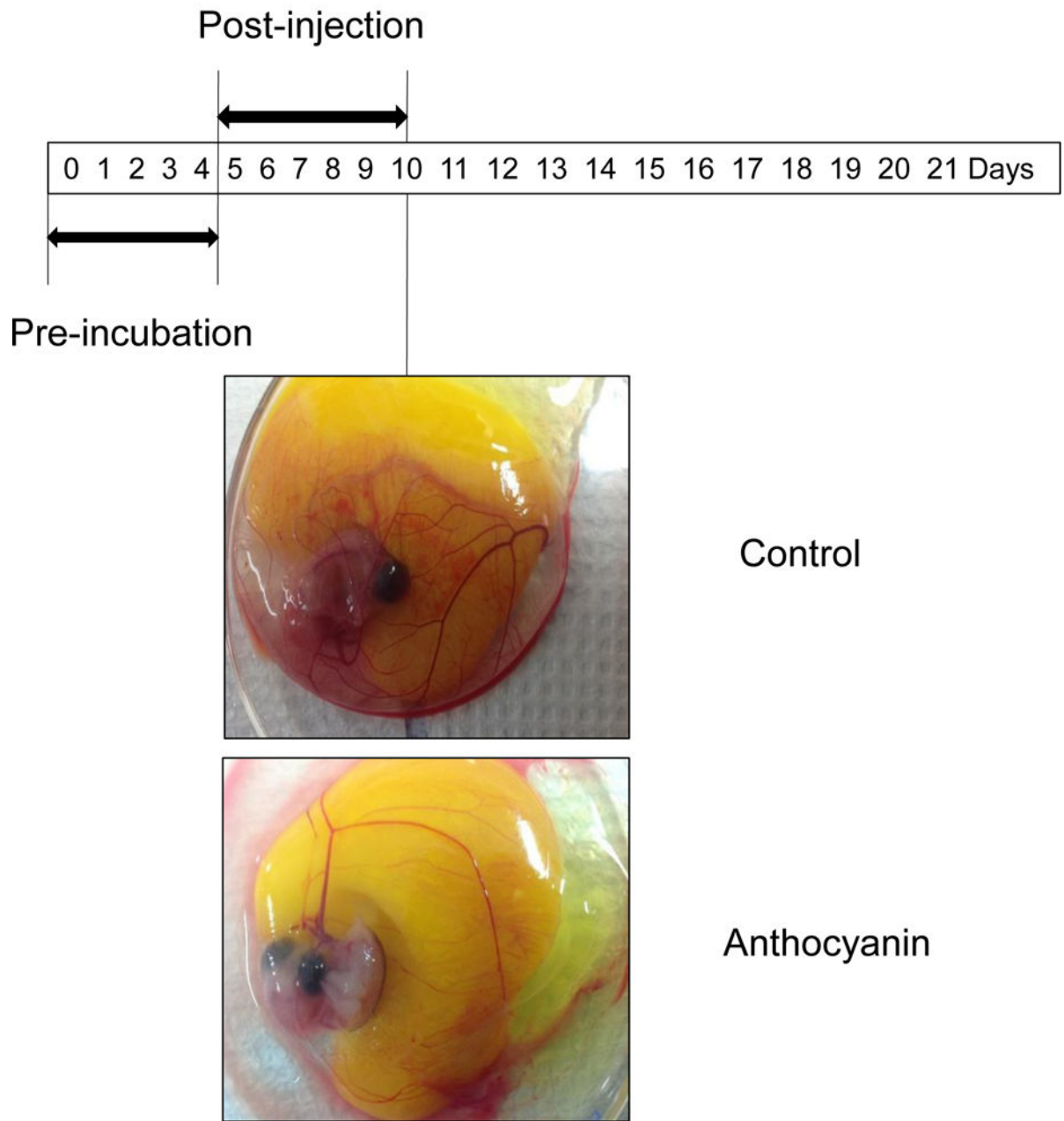
Pre-incubation

Control
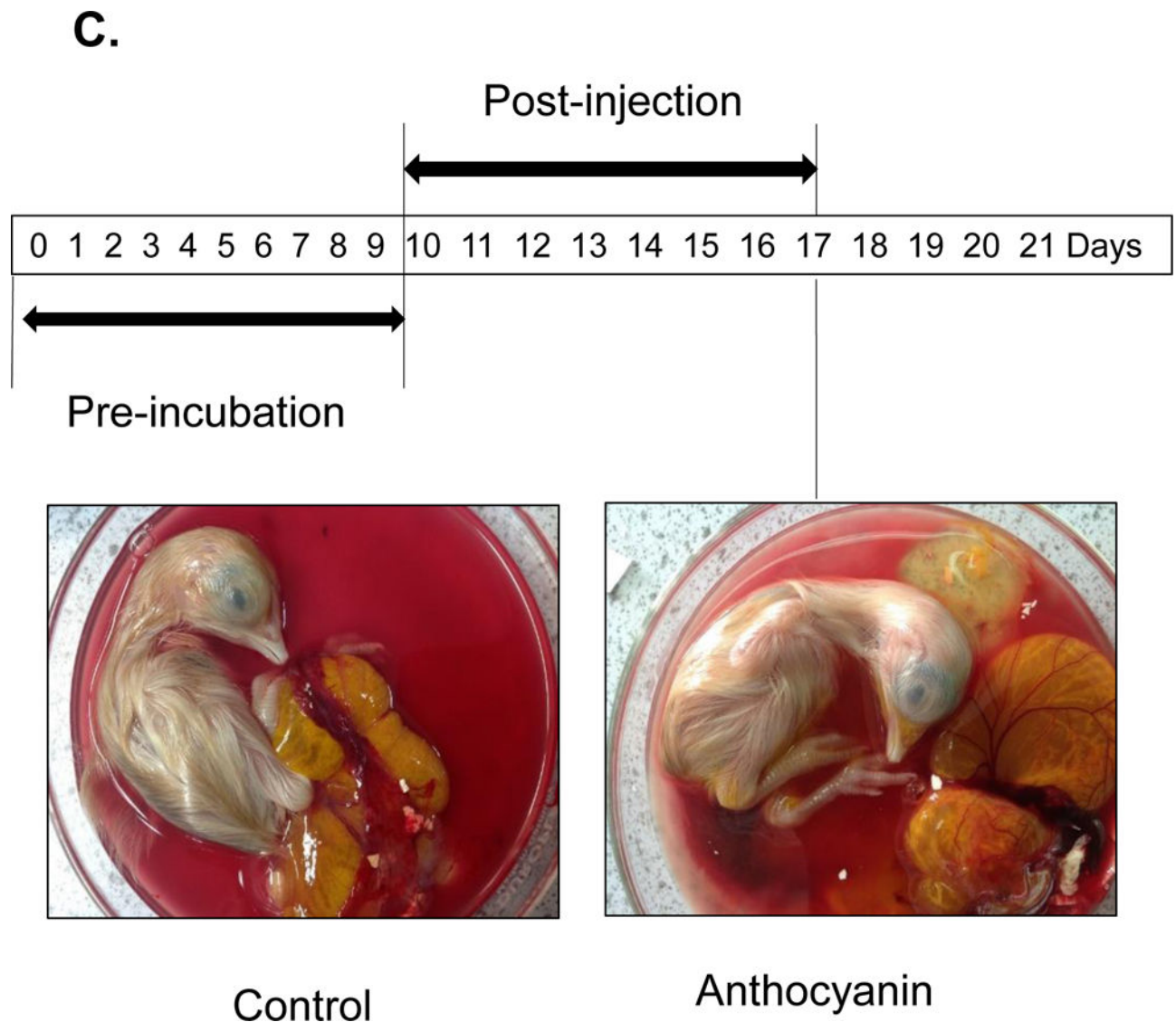
Anthocyanin

Figure 2.
Treatment of chick embryo with anthocyanin-rich extracts of *H. sabdariffa* compared to vehicle control. **A** Pre-incubation of chick embryo for 0–2 days upon injection with 14 μg and 58 μg anthocyanin/38g chick embryo. Early injection (embryonic day ED = 0–2 days) with anthocyanin rich-extracts showed maximum inhibition (>50%) of blood vessel growth, compared to the late injection (pre-incubation ED = 4–7 days before injection). **B** Late injection of anthocyanin rich-extracts 14 μg /chick embryo (pre-incubation ED > 4 days) showed less inhibitory effect on vessel formation. Anthocyanin-rich extracts of *H. sabdariffa* inhibited angiogenic chick embryo in a time and dose-dependent manner. **C.** Late injection of anthocyanin rich-extracts 14 μg /chick embryo (Pre-incubation ED = 9 days) and post-incubation of 8 days showed no difference phenotypically.
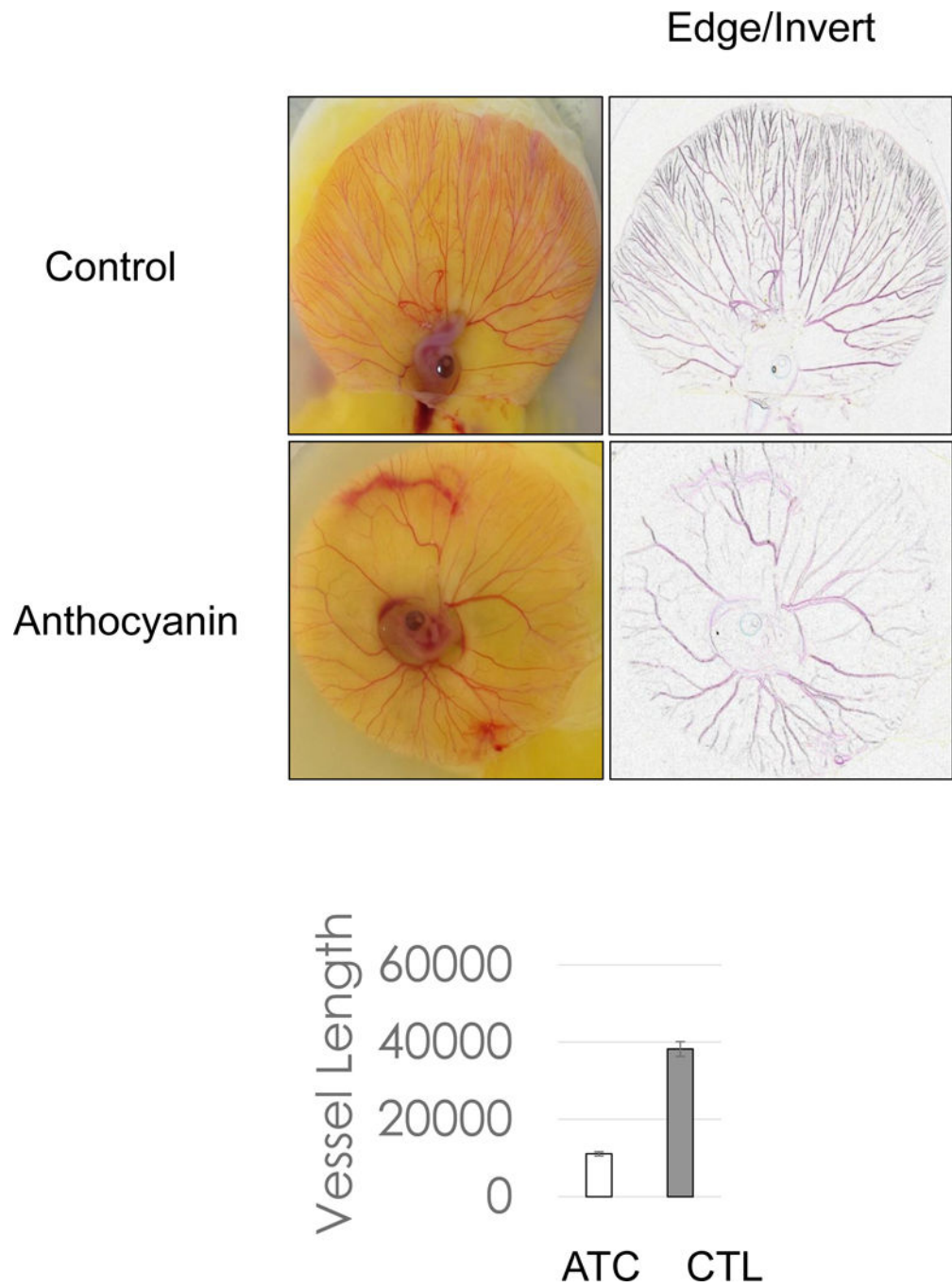
Figure 3.
Early treatment of anthocyanin on chick embryo. Chorioallantoic membrane assay of chick embryo treated with anthocyanin extracts with 14 μg /chick embryo demonstrated that early treatment of anthocyanin extracts with pre-incubation ED = 0 and post-incubation day ED = 4 inhibited vessel growth 75% compared to control.

A.

Angiogenic index: 21 Parameters
Vascular/avascular area
Extremities
Nodes
Junctions
Master junction
Master segments
Master segments length
Meshes
Total meshes area
Pieces=number of segments, isolated elements and branches
Number of segments
Branches
Number of isolated elements
Total length
Total branching length=segments + branches
Total segments length
Total branches length
Total isolated branches length
Branching interval=Total segments length /branches
Mesh index=master segments length /master segments
Mean mesh size
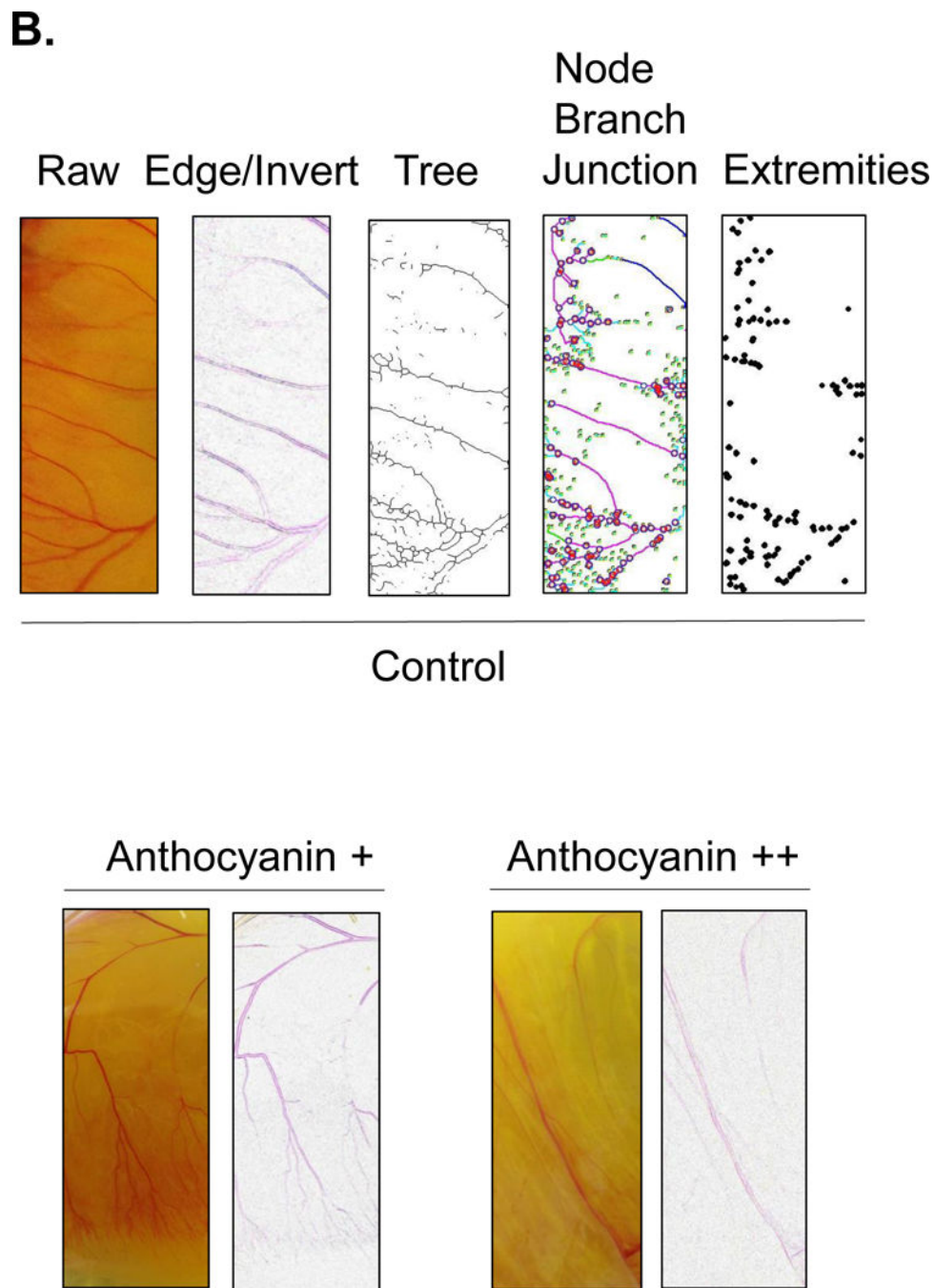
Figure 4.
Angiogenic analysis of chick embryo chorioallantoic membrane. Twenty one angiogenic parameters were examined using Angiogenesis Analyzer macro connected Image J software. Blood vessels were analyzed based on their morphology, including extremities, nodes, twig, segment, junction, branch, master junctions, master segments, master tree, and meshes. The increased concentration of anthocyanin treatment (14 μg and 58 μg/chick embryo) showed dose-dependent inhibition of vessel formation. To calculate the angiogenic index, raw image was converted to find the edge, followed by image inversion. The vessel network

organization was analyzed into a skeleton or tree in a binary image. Nodes that contain pixels with three neighbors as a circular dot, junctions with fusing nodes, and branches (elements delimited by a junction and one extremity) were shown.
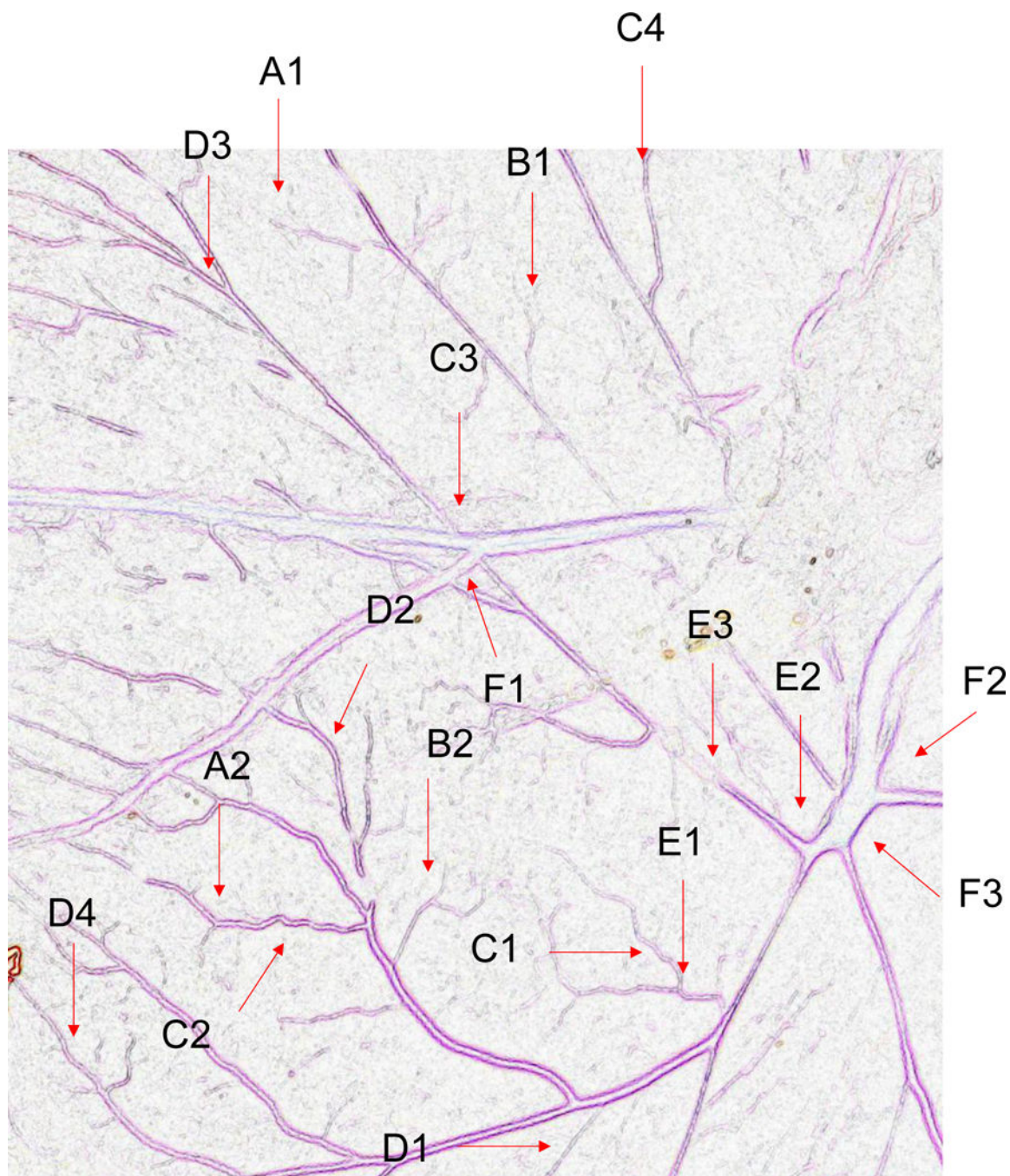
Figure 5.
Angiogenic Analysis showing extremities (A1-B1); nodes identified as 3 neighbor (A2-B2); twig (C1, D1), segment (C2, D2) delimited by two junctions (C3, D3) and branch (C4, D4). E shows a junction implicated only in branch (E1) and master junctions like E2 delimiting master segments (E3). F represents the master tree composed from master segments associated by master junctions delimiting the meshes (F1). Two close master junctions can be fused into a unique master junction (F2) and the underlying segment (F3).
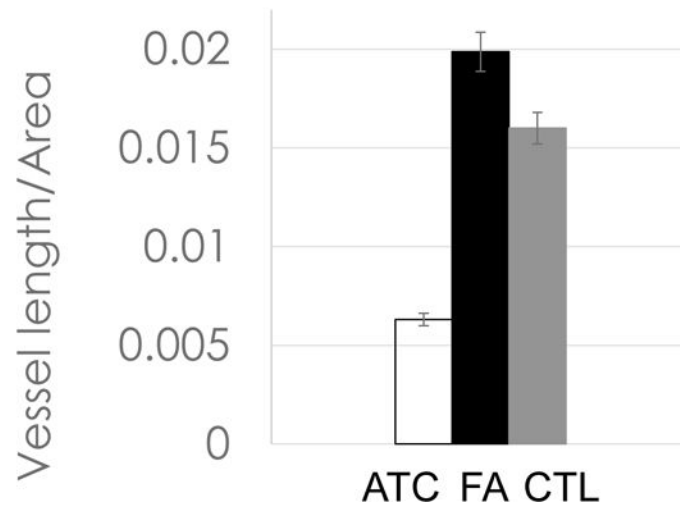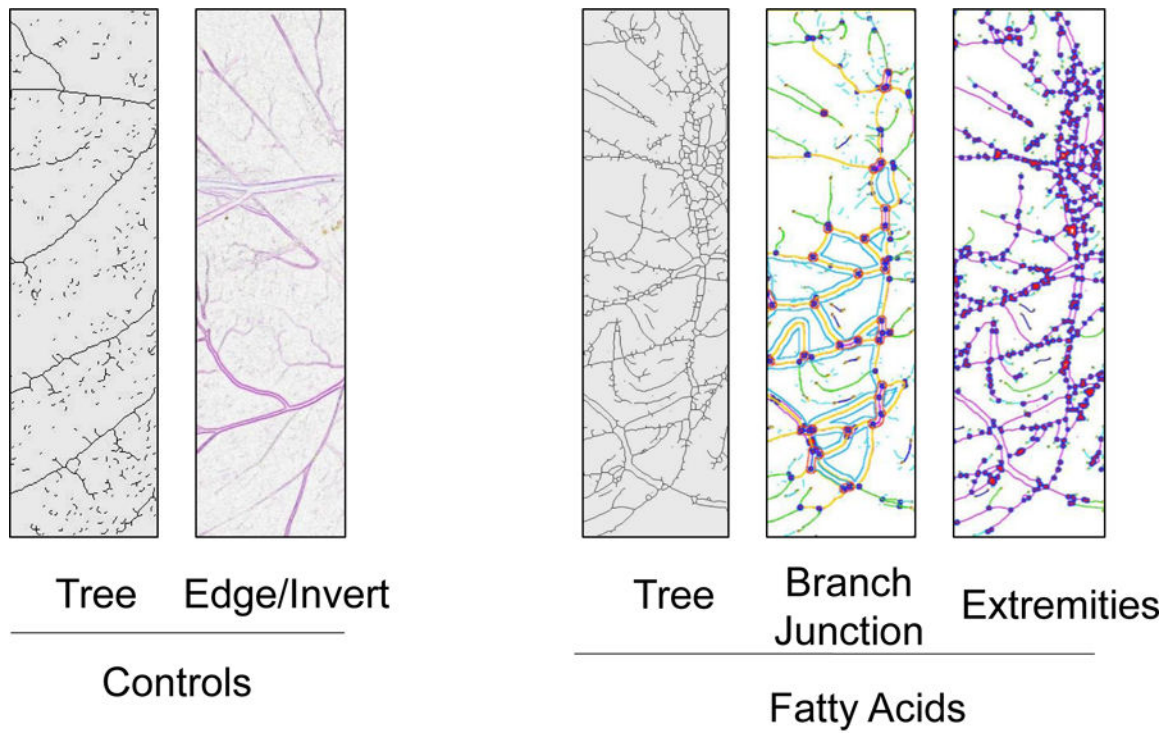
Figure 6.
Comparison of fatty acids vs. anthocyanin. Addition of fatty acid mixtures up-regulated branches, junctions, and extremities. Fatty acid mixtures, including oleic (18:1), linoleic (18:2, w6), linolenic (18:3, w3), palmitic (16:0), palmitoleic (16:1) acid, up-regulated vessel length/area 20–50% compared to control.

A.
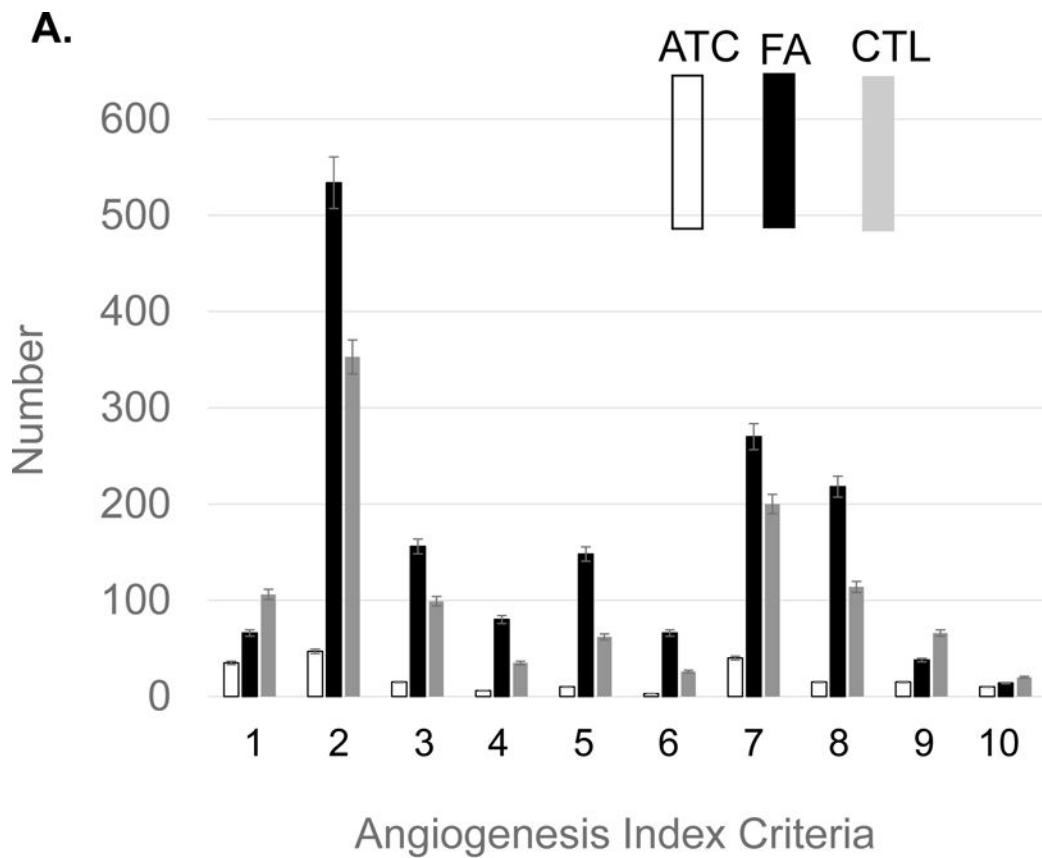
1. Extremities
2. Nodes
3. Junctions
4. Master junction
5. Number of master segments
6. Meshes
7. Total meshes area
8. Number of segments
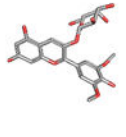9. Branches
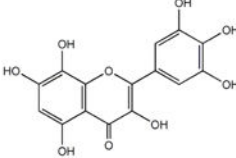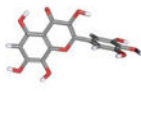10. Number of isolated segments

B.
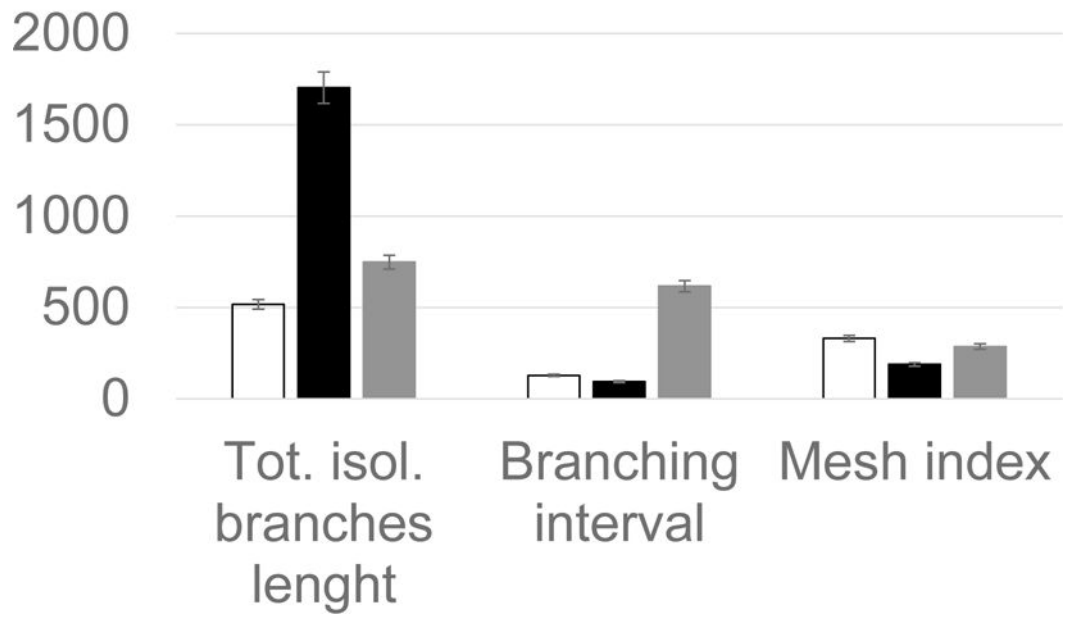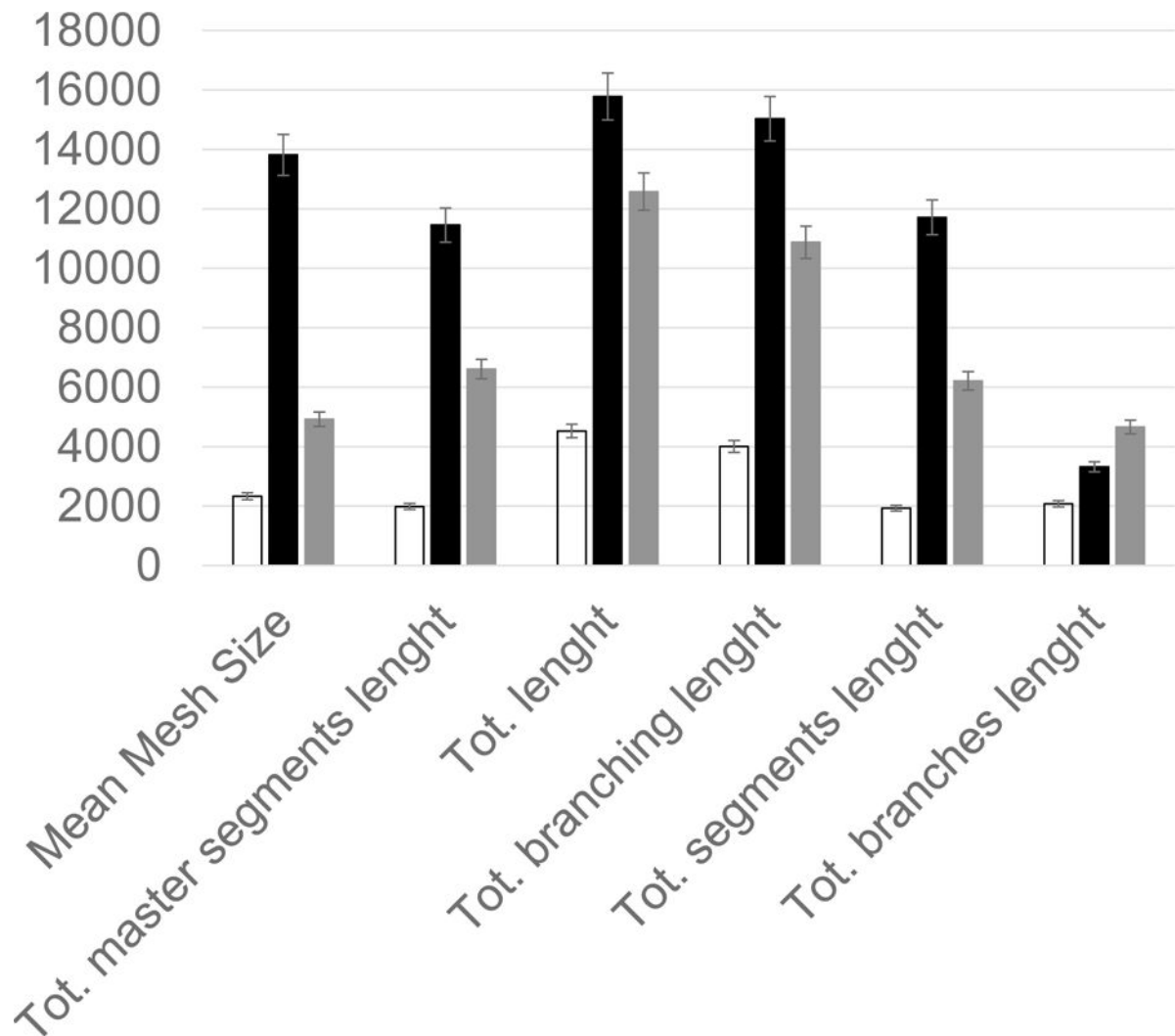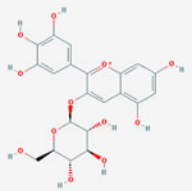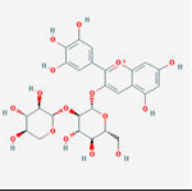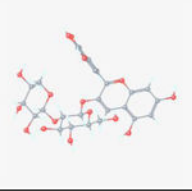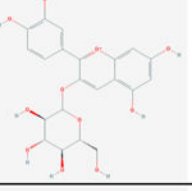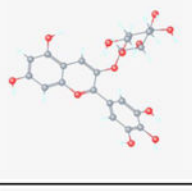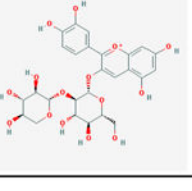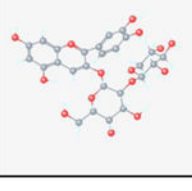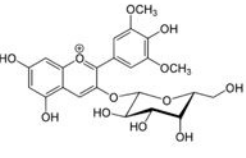
Figure 7.
Statistical computation of angiogenic parameters and comparison of anthocyanin extracts (ATC), fatty acids (FA), and a negative control (CTL). **(A)** Fatty acids up-regulated nodes (2), meshes (6), total meshes area (7), junction (3) and number of master segments (5). Anthocyanin significantly inhibited angiogenic parameters, including nodes, junction, and mesh area. **(B)** Fatty acid mixtures significantly up-regulated total isolated branches length, whereas control showed higher level of branching interval. **(C)** Anthocyanin down-regulated angiogenic index, including total length, branching length, mesh size, and segment length, whereas fatty acids significantly up-regulated total length, total branching length, mean mesh size, total segments length and total master segments length. All values presented are mean ± SD (n = 10). Statistical significance was measured at p< 0.05.

A.

NAME	2D Structure	3D Structure
Delphinidin-3-glucoside		
Delphinidin-3-sambubioside		
Cyanidin-3-glucoside		
Cyanidin-3-sambubioside		
Malvidin-3-galactoside		
Hibiscetin		

B.
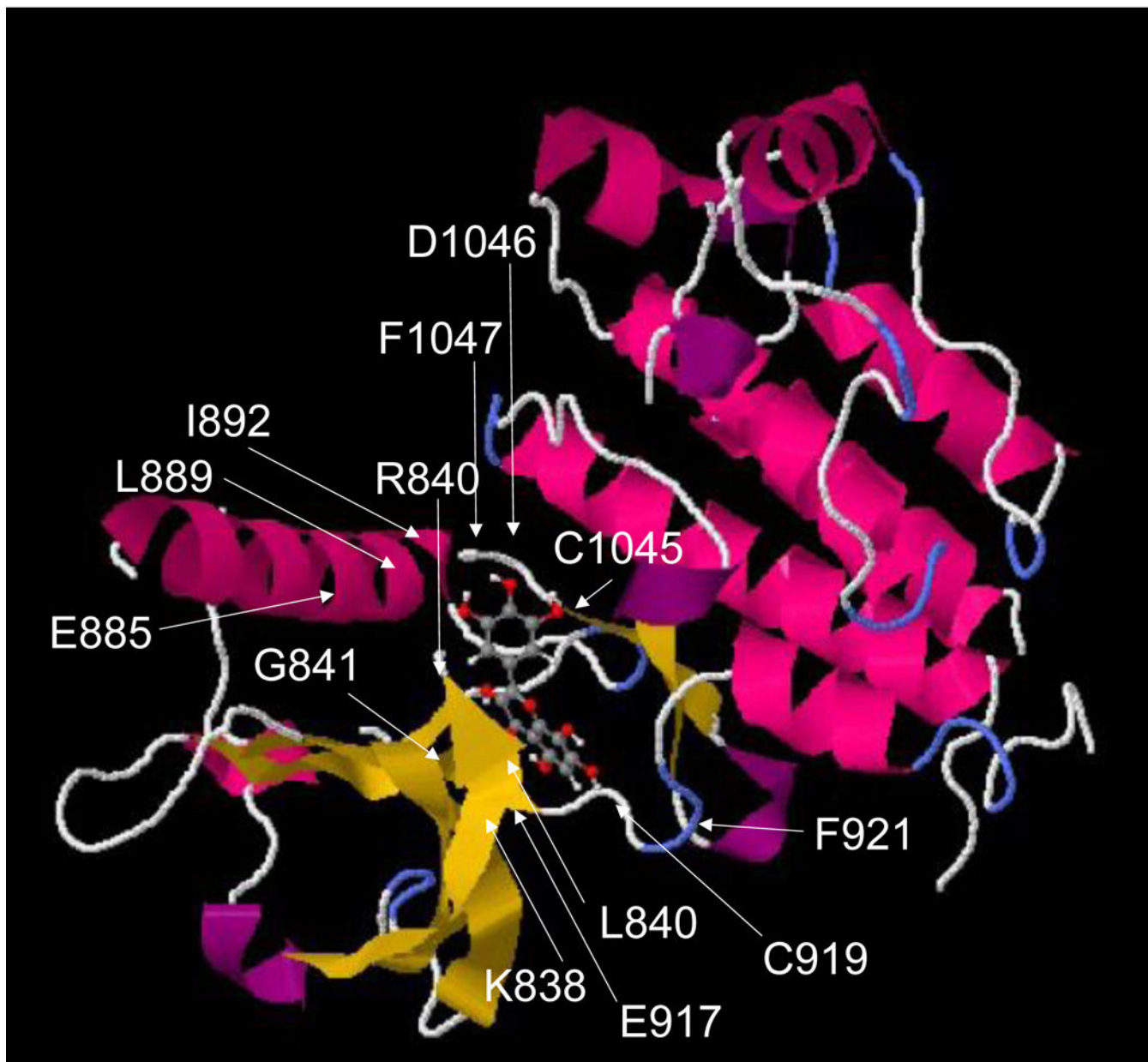
Figure 8.
A. Two-dimensional and 3-dimensional structures of six different anthocyanins, including delphinidin-3-glucoside, delphinidin -3-sambuloside, cyaniding-3-glucoside, cyaniding-3-sambuloside, malvidin-3-galactoside, and hibiscetin, were presented in *Hibiscus sabdariffa* for the molecular binding study. **B.** A 3D model of the protein-ligand interaction was built using the 3D structure VEGFR2 and hibiscetin as a template. VEGFR2 was obtained from the Protein Data Bank (1Y6A).

SwissDock as a protein-ligand docking server was used for ligand-protein interaction studies (http://www.swissdock.ch/docking#). The active site of VEGFR2 and protein structure were examined among seven X-ray diffraction crystal structures (PDB ID = 1Y6A, 1Y6B, 1YWN, 2OH4, 2P2H, 2P21, 2QU5). 257 bindings between VEGFR2 and hibiscetin were calculated with clusters (0–37), elements (0–15), FullFitness (−1588.73 to −1567.50 kcal/mol), binding DG (−8.42 to −6.20 kcal/mol). Swissdock used a hybrid evolutionary algorithm with two fitness functions, with the CHARMM package for energy calculations. The conserved amino acids, including A866, L840, K920, F918, G922, C919, E917, V848, C1045, F1047, L1035, G922, K920, D1046, V916, V899, K868, and E885 in the active site of VEGFR2, were proposed to bind hibiscetin by forming hydrogen bonds (Cys, Glu, Asp), hydrophobic interactions (Ala, Leu, Phe, Val), or π–π interaction (Phe).